Brief Communication

MOLECULAR METABOLISM

ROCK1 regulates insulin secretion from β-cells

Byung-Jun Sung [1], Sung-Bin Lim [1], Won-Mo Yang [2], Jae Hyeon Kim [1], Rohit N. Kulkarni [3], Young-Bum Kim [2,*,5], Moon-Kyu Lee [4,5,]**

ABSTRACT

Objective: The endocrine pancreatic β-cells play a pivotal role in maintaining whole-body glucose homeostasis and its dysregulation is a consistent feature in all forms of diabetes. However, knowledge of intracellular regulators that modulate β-cell function remains incomplete. We investigated the physiological role of ROCK1 in the regulation of insulin secretion and glucose homeostasis.

Methods: Mice lacking ROCK1 in pancreatic β-cells (RIP-Cre; ROCK1$^{loxP/loxP}$, β-ROCK1$^{-/-}$) were studied. Glucose and insulin tolerance tests as well as glucose-stimulated insulin secretion (GSIS) were measured. An insulin secretion response to a direct glucose or pyruvate or pyruvate kinase (PK) activator stimulation in isolated islets from β-ROCK1$^{-/-}$ mice or β-cell lines with knockdown of ROCK1 was also evaluated. A proximity ligation assay was performed to determine the physical interactions between PK and ROCK1.

Results: Mice with a deficiency of ROCK1 in pancreatic β-cells exhibited significantly increased blood glucose levels and reduced serum insulin without changes in body weight. Interestingly, β-ROCK1$^{-/-}$ mice displayed a progressive impairment of glucose tolerance while maintaining insulin sensitivity mostly due to impaired GSIS. Consistently, GSIS markedly decreased in ROCK1-deficient islets and ROCK1 knockdown INS-1 cells. Concurrently, ROCK1 blockade led to a significant decrease in intracellular calcium and ATP levels and oxygen consumption rates in isolated islets and INS-1 cells. Treatment of ROCK1-deficient islets or ROCK1 knockdown β-cells either with pyruvate or a PK activator rescued the impaired GSIS. Mechanistically, we observed that glucose stimulation in β-cells greatly enhanced ROCK1 binding to PK.

Conclusions: Our findings demonstrate that β-cell ROCK1 is essential for glucose-stimulated insulin secretion and for glucose homeostasis and that ROCK1 acts as an upstream regulator of glycolytic pyruvate kinase signaling.

Keywords ROCK1; Insulin secretion; Beta cells; Hyperglycemia; Pyruvate kinase; Diabetes

1. INTRODUCTION

Diabetes is a rapidly growing health problem worldwide as evidenced by increasing morbidity and mortality and the economic burden on society [1,2]. Diabetes is characterized by hyperglycemia, peripheral insulin resistance, and impaired β-cell function [3,4]. Pancreatic β-cells directly contribute to the regulation of systemic glucose balance by releasing insulin primarily in response to glucose, although other nutrients such as fatty and amino acids can also enhance insulin secretion [5,6]. Impaired glucose-stimulated insulin secretion secondary to defects in signaling pathways has been reported as a contributing factor to the development of systemic glucose intolerance and overt diabetes [7,8]. Therefore, identifying molecular mediators that underlie the precise regulation of glucose-induced insulin secretion is of great significance.

Glucose is the principal stimulator of insulin secretion from β-cells acting via the glycolytic pathway [9]. Pyruvate kinase (PK), an enzyme involved in the terminal step of glycolysis, catalyzes the transfer of a phosphate group and converts phosphoenolpyruvate and adenosine diphosphate (ADP) to produce pyruvate and adenosine triphosphate (ATP) [10]. Recent studies demonstrate that activation of PK promotes insulin secretion during glucose stimulation in INS-1 β-cells, mouse, and human islets [11]. Furthermore, PK activators can enhance insulin secretion from normal, high-fat diet-fed or Zucker diabetic fatty rats and diabetic humans [12], indicating the significance of PK in regulating β-cell secretory function.

ROCK1 (Rho-kinase 1; Rho-associated coiled-coil containing kinase 1) is involved in the pathogenesis of metabolic-related diseases, including hypertension, arteriosclerosis, Alzheimer's disease, and diabetes [13–15]. Emerging evidence shows that peripheral ROCK1

[1]Division of Endocrinology and Metabolism, Department of Medicine, Samsung Medical Center, Sungkyunkwan University School of Medicine, Seoul, South Korea [2]Division of Endocrinology, Diabetes and Metabolism, Beth Israel Deaconess Medical Center and Harvard Medical School, Boston, MA, USA [3]Islet Cell and Regenerative Medicine, Joslin Diabetes Center, Department of Medicine, Beth Israel Deaconess Medical Center, Harvard Stem Cell Institute, and Harvard Medical School, Boston, MA, USA [4]Division of Endocrinology and Metabolism, Department of Internal Medicine, Nowon Eulji University Hospital, Eulji University School of Medicine, Seoul, South Korea

[5] Young-Bum Kim and Moon-Kyu Lee contributed equally to this work.

*Corresponding author. Division of Endocrinology, Diabetes, and Metabolism, Beth Israel Deaconess Medical Center, 330 Brookline Avenue, Boston, MA 02215, USA.

**Corresponding author. Division of Endocrinology and Metabolism, Department of Internal Medicine, Nowon Eulji University Hospital, 68 Hangeulbiseok-ro, Seoul, South Korea.

E-mails: sungbyungjun@gmail.com (B.-J. Sung), sb9205@naver.com (S.-B. Lim), wyang10@bidmc.harvard.edu (W.-M. Yang), jaehyeon@skku.edu (J.H. Kim), Rohit.Kulkarni@joslin.harvard.edu (R.N. Kulkarni), ykim2@bidmc.harvard.edu (Y.-B. Kim), leemk4132@eulji.ac.kr (M.-K. Lee).

Received August 26, 2021 • Revision received October 21, 2022 • Accepted October 26, 2022 • Available online 29 October 2022

https://doi.org/10.1016/j.molmet.2022.101625

controls insulin-mediated glucose metabolism and insulin signaling, whereas brain ROCK1 plays a dominant role in regulating feeding behavior and body-weight homeostasis [16–24]. In the liver, ROCK1 is necessary for the development of diet-induced insulin resistance and hepatic steatosis in rodents and humans [25]. Although a study reported that chemical inhibition of ROCK promotes glucose-stimulated insulin secretion in primary pancreatic β-cells [26], the precise pathways and signaling proteins that mediate the effects are virtually unexplored. Furthermore, a lack of ROCK isoform selectivity and incomplete understanding of their respective specificities makes it difficult to interpret studies with inhibitors [27–29].

In the current study, we investigated the role of ROCK1 in directly regulating glucose metabolism by studying mice lacking ROCK1 in pancreatic β-cells in vivo and ROCK1-deficient islets *ex vivo* as well as cultured β-cell lines *in vitro*, with particular emphasis on glucose-stimulated insulin secretion and whole-body glucose homeostasis.

2. MATERIALS AND METHODS

2.1. Animal care

All animal care and experimental procedures were conducted in accordance with the National Institute of Health's Guide for the Care and Use of Laboratory Animals and approved by the Institutional Animal Care and Use Committee of Samsung Medical Center (Seoul, Republic of Korea) and Beth Israel Deaconess Medical Center (Boston, MA). Mice were housed at 22–24 °C on a 12 h light–dark cycle and allowed *ad libitum* access to standard chow (PicoLab® Rodent Diet 5053, LabDiet, St. Louis, MO) and water.

2.2. Generation of RIP-Cre; ROCK1$^{loxP/loxP}$ mice

Mice bearing a loxP-flanked ROCK1 allele (ROCK1$^{loxP/loxP}$) were generated and maintained as previously described [22]. Mice lacking ROCK1 in pancreatic β-cells (β-ROCK1$^{-/-}$, RIP-Cre; ROCK1$^{loxP/loxP}$) were generated by breeding ROCK1$^{loxP/loxP}$ mice with RIP-Cre transgenic mice (The Jackson lab, Stock No: 003573). ROCK1$^{loxP/loxP}$ mice were used as controls. All mice were maintained on a mixed genetic background (129Sv and C57BL/6).

2.3. Metabolic parameter measurements

Mice were weighed weekly from 5 weeks of age onwards. For daily food intake, 14-week-old males were individually housed for 1 week prior to the start of food intake measurements. Subsequently, food intake was measured over a 7-day period. Blood was collected via the tail from either randomly fed or overnight-fasted mice. Blood glucose was measured using a glucose meter (Roche, Basel, Switzerland), serum insulin by ELISA (Mercodia, Uppsala, Sweden), and glucagon by ELISA (R&D Systems, Minneapolis, MN, USA).

2.4. Oral glucose tolerance and insulin tolerance test

For the oral glucose tolerance test (OGTT), 8, 20, and 48-week-old males were fasted for 6 h, and blood glucose was measured before and 30, 60, 90, and 120 min after administrating glucose by gavage (2 g/kg body weight). For the insulin tolerance test (ITT), 8, 20, and 48-week-old males were fasted for 6 h, and blood glucose was measured before and 15, 30, 60, 90, and 120 min after an intraperitoneal injection of human insulin (0.75 IU/kg body weight: Humulin R, Eli Lilly). Blood glucose was measured using a glucose meter (Roche). The area under the curve for glucose was calculated using the trapezoidal rule for OGTT [30].

2.5. Measurement of β-cell numbers and islet insulin content

Pancreas sections (5 μm thick) were immunostained for insulin (guinea pig anti-insulin pig from Abcam, 1:1000, overnight at 4 °C, secondary antibody; Alexa Fluor 647-conjugated anti-guinea pig from Thermo Fisher Scientific, 1:500, 1 h at room temperature) and nuclei were stained with DAPI (MilliporeSigma) in fluorescent mounting medium (Dako). The number of insulin^{+} β-cells were counted in a random manner by a single observer using a microscope (Olympus Corp.). Samples were blinded to the observer. At least 100 cells were counted per mouse. Insulin levels in islets were measured by ELISA (Mercodia) according to the manufacturer's instructions.

2.6. Pancreatic islet isolation

Pancreases were rapidly dissected after intra-ductal injection from 9 to 10-week-old male mice and islets were isolated by digesting the pancreas with collagenase P (Roche, Basel, Switzerland) and purified using a Ficoll gradient (Merck Biochrom, Billerica, MA) [31]. After isolation, the islets were cultured for 24 h at 37 °C and size-matched islets were hand-picked using an inverted microscope under sterile conditions. Ten or thirty size-matched islets per individual experiment (per genotype) were used.

2.7. Perifusion analysis

The isolated islets or β-cell lines (INS-1 and MIN6 cell) were pre-incubated in a HEPES-KRB buffer containing 3.3 mM glucose for 30 min at 37 °C and placed in a 0.2 μm syringe filter. The filter was connected to a peristaltic pump and the flow rate was adjusted to 2 or 5 ml/min. Fractions were serially collected at 5 min intervals for 30 min, 1 min intervals for 10 min, 2 min intervals for 50 min, and 5 min intervals for 30 min. Fractions were appropriately diluted and measured for insulin by ELISA (Mercodia).

2.8. Glucose-stimulated insulin secretion (GSIS)

The isolated islets or β-cell lines (INS-1 and MIN6 cell) were pre-incubated with a KRB buffer containing 3.3 mM glucose at 37 °C for 120 min and incubated with either 3.3 mM or 16.7 mM glucose in a KRB buffer at 37 °C for 60 min in the presence or absence of sodium pyruvate (10 mM, MilliporeSigma), TEPP-46 (10 μM, MilliporeSigma), or exendin-4 (20 nM, MilliporeSigma). Insulin levels in the media were determined by ELISA (Mercodia).

2.9. Cell culture

The INS-1 832/13 cells (gift from C. Newgard PhD, Duke University) were cultured in RPMI-1640 (Thermo Fisher Scientific) supplemented with 10% fetal bovine serum (FBS, Thermo Fisher Scientific) and 1% penicillin-streptomycin (P/S, Thermo Fisher Scientific) and HEPES. The MIN6 mouse insulinoma cells were cultured in DMEM supplemented with 15% FBS (Thermo Fisher Scientific) and 1% P/S. The MIN6 cells (Addexbio) were cultured in AddexBio advanced medium (Addexbio) supplemented with 15% FBS, 0.05 mM 2-mercaptoethanol (Thermo Fisher Scientific), and 1% P/S. The NIT1 mouse insulinoma cells (ATCC, American Type Culture Collection) were cultured in Ham's F12K (ATCC) supplemented with 10% FBS and 1% P/S. The HEK293 human embryonic kidney cells were cultured in DMEM supplemented with 10% FBS and 1% P/S. The Chinese hamster ovary (CHO) cells were cultured in Ham's F-12 (Thermo Fisher Scientific) supplemented with 10% FBS and 1% P/S. All cells were cultured at 37 °C in an atmosphere of 5% CO_2.

2.10. Transfection

INS-1 or MIN6 cells were transiently transfected with small interfering RNA (siRNA) using Lipofectamine 2000 (Thermo Fisher Scientific) according to the manufacturer's instructions. Cells were used for studies 48 h after transfection. The siRNA sequence for ROCK1 (Bioneer, Daejeon, South Korea) was 5′-UCCAAGUCACAAGCAGACAAGGAUU-3′ as described [20]. Scramble siRNA was used as an experimental control (Bioneer). MIN6, HEK293, or CHO cells were transiently transfected with pAV-CAG-ROCK1 (Vigene Biosciences, Rockville, MD) and pEGFP-C1-PKM2 (Addgene, Watertown, MA) using Lipofectamine 3000 (Thermo Fisher Scientific) according to the manufacturer's instructions. The cells were used for studies 48 h after transfection.

2.11. Measurement of ATP and calcium levels

The isolated islets or INS-1 cells were preincubated in 3.3 mM glucose and subsequently incubated in 16.7 mM glucose for 60 min at 37 °C. For measuring ATP levels, islets or cells were washed with PBS and the bioluminescence reaction was initiated by adding BacTiter-Glo™ reagent (Promega, Madison, WI) and maintained for 5 min at room temperature. Bioluminescence was determined by a GloMax Multi Microplate Multi Reader (Promega). For measuring calcium levels, the freshly isolated islets or cells were preincubated with 3.3 mM glucose for 120 min and incubated with 16.7 mM glucose treated with Fluo-4 direct calcium reagent solution containing 2.5 mM probenecid (F10472, Invitrogen) for 60 min at 37 °C. Fluorescence was measured at an excitation wavelength of 494 nm and emission wavelength at 516 nm by a GloMax Multi Microplate Multi Reader (Promega) [32].

2.12. Oxygen consumption rate (OCR) measurements

The isolated islets or INS-1 cells were preincubated with 3.3 mM glucose for 120 min and incubated with 16.7 mM glucose for 60 min at 37 °C. The OCR was determined using the Seahorse Extracellular Flux (XF-96) analyzer (Seahorse Bioscience). The OCR were calculated by normalizing the protein content for the XF-96 measurement [33].

2.13. Pyruvate and PK measurements

The isolated islets or INS-1 cells were preincubated with 3.3 mM glucose for 120 min and incubated with 16.7 mM glucose for 60 min. Pyruvate levels in islets and INS-1 cells were measured by the Pyruvate Assay Kit (abcam, #ab65342, Cambridge, United Kingdom) according to the manufacturer's instructions. PK activity in INS-1 cells was measured by the Pyruvate Kinase Assay Kit (Abcam, #ab83432) according to the manufacturer's instructions.

2.14. Proximity ligation assay (PLA)

INS-1, MIN6, or NIT1 cell lines were treated with or without fasudil (10 μM) for 1 h and stimulated with high (16.7 mM) glucose for 15 min. Cells were incubated with primary antibodies against ROCK1 (1:100, Cat #: sc-17794, Santa Cruz Biotechnology, Dallas, TX, USA) and PK (1:100, Cat #: ab38237, Abcam) overnight at 4 °C. PLA was performed as described previously [34]. PLA was performed using the Duolink® In Situ Detection Reagents Red with Duolink® In Situ PLA probe anti-rabbit PLUS and anti-mouse MINUS (MilliporeSigma). The nuclei of cells were stained using Duolink® In Situ Mounting Medium with DAPI (MilliporeSigma). Images were captured by a fluorescence microscope (Leica DMi8, Leica) and analyzed by ImageJ (NIH).

2.15. Immunoprecipitation assay

The cell lysates (100 μg) were subjected to immunoprecipitation with 1 μg HA (Cat #: 3724, Cell Signaling Technology) or normal rabbit IgG (Cat #: 2729, Cell Signaling Technology) coupled to Dynabead protein A/G (Thermo Fisher Scientific) overnight at 4 °C. The immunoprecipitants were washed four times with lysis buffer, and then were eluted by 1X Novex™ Tris-Glycine SDS sample buffer (Thermo Fisher Scientific) with 1X NuPAGE™ Sample Reducing Agent (Thermo Fisher Scientific) for 10 min at 100 °C.

2.16. Immunoblotting analysis

Tissue lysates (30 μg protein) or immunoprecipitated samples were resolved by SDS—PAGE and transferred to nitrocellulose membranes (Bio-Rad Laboratories, Hercules, CA). The membranes were incubated with antibodies against ROCK1 (Cat#: sc-17794, Santa Cruz Biotechnology), ROCK2 (Cat#: sc-5561, Santa Cruz Biotechnology), HA, or β-actin (Cat#: sc-130065, Santa Cruz Biotechnology). The membranes were washed and incubated with secondary antibodies (Cat#: SC-2004 or SC-2005, Santa Cruz Biotechnology). The bands were visualized with SuperSignal Chemiluminescent Substrates (Thermo Fisher Scientific).

2.17. Electron microscopy

Pancreases from ROCK1$^{loxP/loxP}$ and β-ROCK1$^{-/-}$ mice fed high glucose were fixed in 2% glutaraldehyde for 12 h. An electron microscopic analysis of docked granules was performed on the pancreas sections and quantitated as described previously [35].

2.18. Statistical analyses

Data are presented as means ± SEM and individual data points are plotted. Unpaired Student's 't' tests were used to compare two groups. For comparisons involving more than two groups, one-way analysis of variance (ANOVA) was performed with post-hoc tests and Fisher's PLSD tests. Repeated measures two-way ANOVA was performed for GTT, ITT, and GSIS. When intervention or interaction (intervention-by-time) was significant by repeated measures two-way ANOVA, post hoc analyses were performed using the SPSS program (SPSS version 18.0, SPSS, Inc., Chicago, IL) for multiple comparisons. All reported p values were two-sided unless otherwise described. Differences were considered significant at $P < 0.05$.

3. RESULTS

3.1. Selective deletion of ROCK1 in pancreatic β-cells leads to hyperglycemia and impaired glucose-stimulated insulin secretion

We confirmed that ROCK1 expression in pancreatic islets was decreased ~65% in β-ROCK1$^{-/-}$ mice compared with ROCK1$^{loxP/loxP}$ (control) mice (Control vs. β-ROCK1$^{-/-}$ mice; 100 ± 5.9 vs. 34.9 ± 2.1%, n = 3), whereas its expression in hypothalamus and peripheral tissues was not different between genotypes (Supplementary Fig. 1). Furthermore, a lack of significant expression of ROCK2 in the islets suggested a lack of compensation between isoforms (Supplementary Fig. 1). Body weight (Figure 1A) and daily food intake and accumulated food intake (7 days) were similar between groups (Figure 1B and C). However, β-ROCK1$^{-/-}$ mice displayed hyperglycemia compared with control mice starting at 5 weeks of age, peaked at ~12 weeks, and remained high throughout the 42 week period of the study (Figure 1D). Serum insulin levels in β-ROCK1$^{-/-}$ mice significantly decreased (~54%) compared with ROCK1$^{loxP/loxP}$ mice, whereas serum glucagon levels were comparable between groups (Figure 1E and F). Importantly, the islet perifusion analysis showed a marked decrease in both the 1st and 2nd phases of insulin secretion in response to glucose stimulation in β-ROCK1$^{-/-}$ mice (Figure 1G, Supplementary Fig. 2A). The *ex vivo* statically incubated

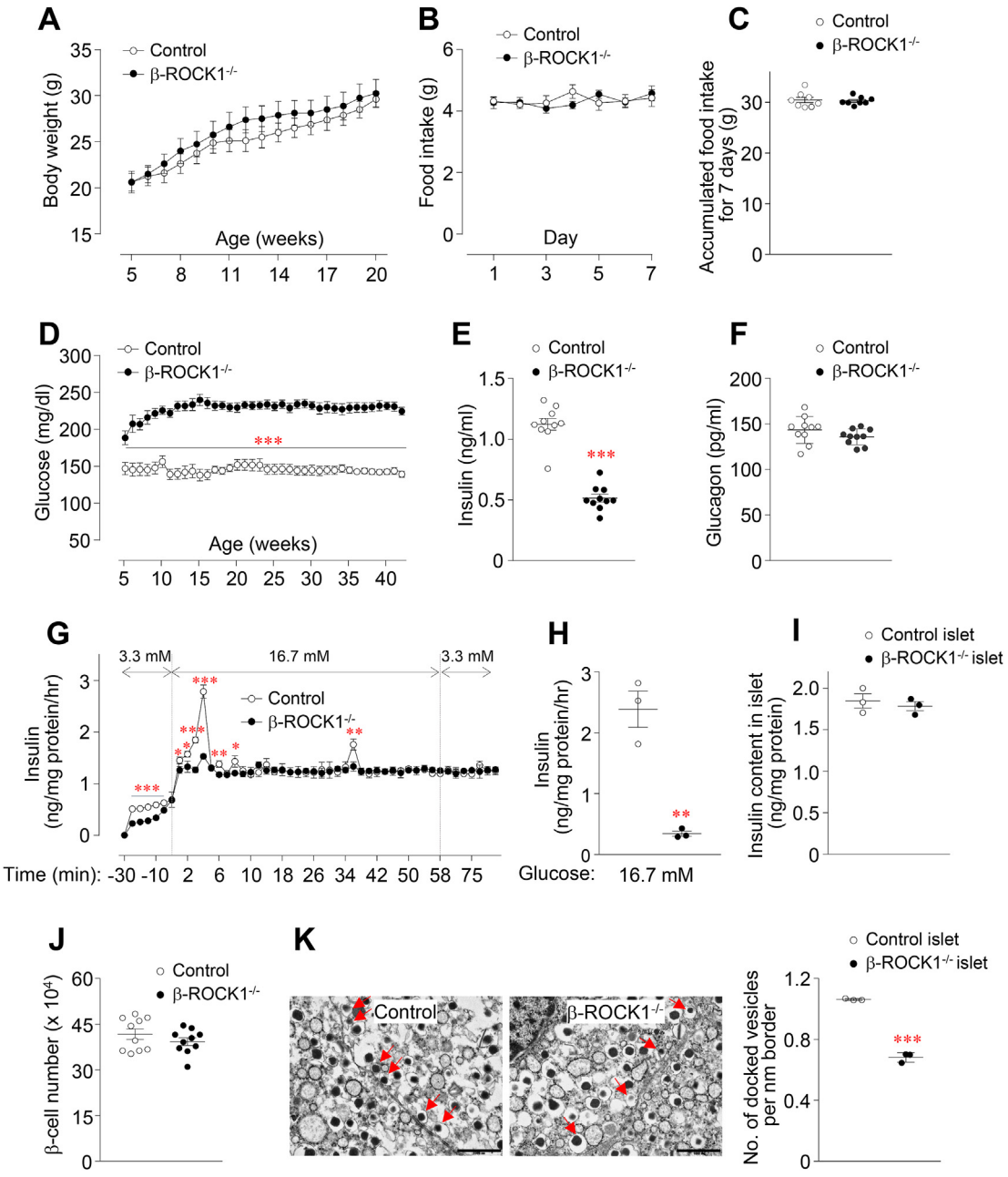

Figure 1: Loss of ROCK1 in pancreatic β-cells leads to hyperglycemia and impaired glucose-stimulated insulin secretion. (A) Body weight (n = 8), (B) daily food intake (n = 8), (C) accumulated food intake for 7 days (n = 8), (D) blood glucose (n = 10), (E) serum insulin (n = 10), and (F) serum glucagon (n = 10) were measured in male control and β-ROCK1$^{-/-}$mice. Serum parameters and fat depots were measured from overnight-fasted mice at 9—10 weeks of age. Food intake was measured at 14 weeks of age for 1 week. (G) Perifusion analysis for glucose-stimulated insulin secretion (GSIS) was performed in isolated islets from male control and β-ROCK1$^{-/-}$ mice (n = 3). Ten size-matched islets per individual experiment (per genotype) were used for perifusion experiments. N represents an individual experiment. (H) GSIS, (I) insulin content, and (J) β-cell number were measured in isolated islets from male control and β-ROCK1$^{-/-}$ mice (n = 10). (K) Insulin vesicles associated with the plasma membrane were assessed in isolated islets from male control and β-ROCK1$^{-/-}$ mice. Pancreatic sections were obtained from 3 mice per genotype (n = 3) for measuring insulin vesicles. The arrows indicate membrane-docked vesicles. The scale bar represents 1 μm. The bar graph shows the quantitation of the number of vesicles docked to the plasma membrane. All graphs represent means or individual values ± SEM. *$p < 0.05$, **$p < 0.01$, ***$p < 0.001$ vs control by two-sided Student's t-test.

islet experiments further confirmed these observations (see Figure 1H). However, ROCK1 deletion in pancreatic β-cells had no significant effects on insulin content or β-cell numbers (Figure 1I and J).

The proximity of insulin granules to the cell surface of β-cells is thought to especially impact the magnitude of the 1st phase insulin release [36,37]. Electron microscopy analysis showed the number of secreted granules close to the cell membrane in β-cells of β-ROCK1$^{-/-}$ mice reduced by 32% compared with β-cells in control mice (Figure 1K, left and right panels), indicating that ROCK1 activation is important in the docking process of insulin granules to the β-cell membrane. Collectively, these results suggest ROCK1 activation in pancreatic β-cells is involved in the regulation of insulin secretion in vivo.

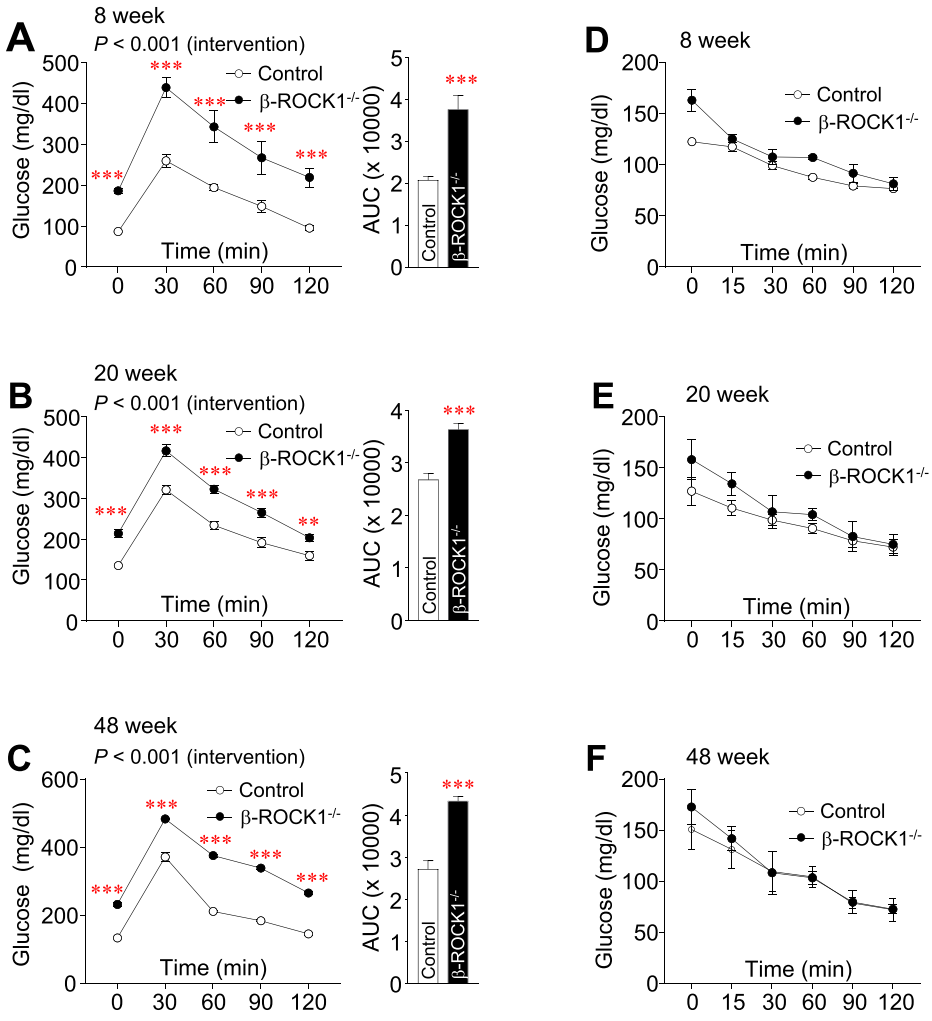

Figure 2: ROCK1 deletion from pancreatic β-cells causes glucose intolerance but not insulin resistance. (A) Oral glucose tolerance test (OGTT) at 8 weeks of age (n = 4), (B) OGTT at 20 weeks of age (n = 11 for control, n = 17 for β-ROCK1−/−), and (C) OGTT at 48 weeks of age (n = 12 for control, n = 14 for β-ROCK1−/−) were performed in male control and β-ROCK1−/−mice. (D) Insulin tolerance test (ITT) at 8 weeks of age (n = 4), (E) ITT at 20 weeks of age (n = 11), and (F) ITT at 48 weeks of age (n = 5) were performed in male control and β-ROCK1−/−mice. Area under the curve (AUC) for GTT was calculated. All graphs represent means ± SEM. P values (intervention) for GTT were evaluated by repeated measures two-way ANOVA and P values for AUCs were evaluated by two-sided Student's t-test. $^{**}p < 0.01$, $^{***}p < 0.001$ vs control mice by repeated measures two-way ANOVA.

3.2. Mice lacking ROCK1 in pancreatic β-cells are glucose intolerant but not insulin resistant

β-ROCK1$^{-/-}$ mice showed impaired glucose tolerance by 8 weeks of age, as revealed by an increased area under the glucose curve during OGTT (Figure 2A). While the β-ROCK1$^{-/-}$ mice continued to exhibit glucose intolerance as they aged, the intolerance did not worsen (Figure 2B and C). This effect is most likely due to impaired glucose-stimulated insulin secretion and is independent of changes in body weight or insulin sensitivity (Figure 2D—F). Glucose tolerance measured by ipGTT was normal among RIP-Cre, RIP-WT, and ROCK1$^{loxP/loxP}$ mice at 10 weeks of age (Supplementary Fig. 3A). In addition, at 25 weeks of age, oral glucose tolerance was not different between RIP-Cre and ROCK1$^{loxP/loxP}$ mice (Supplementary Fig. 3B). Together, these data highlight the necessity of ROCK1 in regulating β-cell function without impacting insulin sensitivity.

3.3. Inhibition of ROCK1 impairs glucose-stimulated insulin secretion in INS-1 cells and MIN6 cells

We measured GSIS in INS-1 and MIN6 cell lines transfected with ROCK1 siRNA to further determine whether ROCK1 directly regulates insulin secretion in cultured β-cells. We confirmed that ROCK1 siRNA significantly reduced ROCK1 mRNA levels (Supplementary Fig. 2A). Consistent with the in vivo results, inhibition of ROCK1 significantly reduced both phases of insulin secretion measured during glucose perifusion in INS-1 cells (Figure 3A, Supplementary Fig. 3B) and MIN6 cells (Supplementary Fig. 4B). GSIS markedly decreased when ROCK1 expression was suppressed (Figure 3B, Supplementary Fig. 4C), whereas insulin content was relatively normal in the cell lines (Figure 3C, Supplementary Fig. 4D). These data, combined with the results of in vivo insulin secretion, demonstrate that ROCK1 activation is necessary to regulate glucose-stimulated insulin secretion.

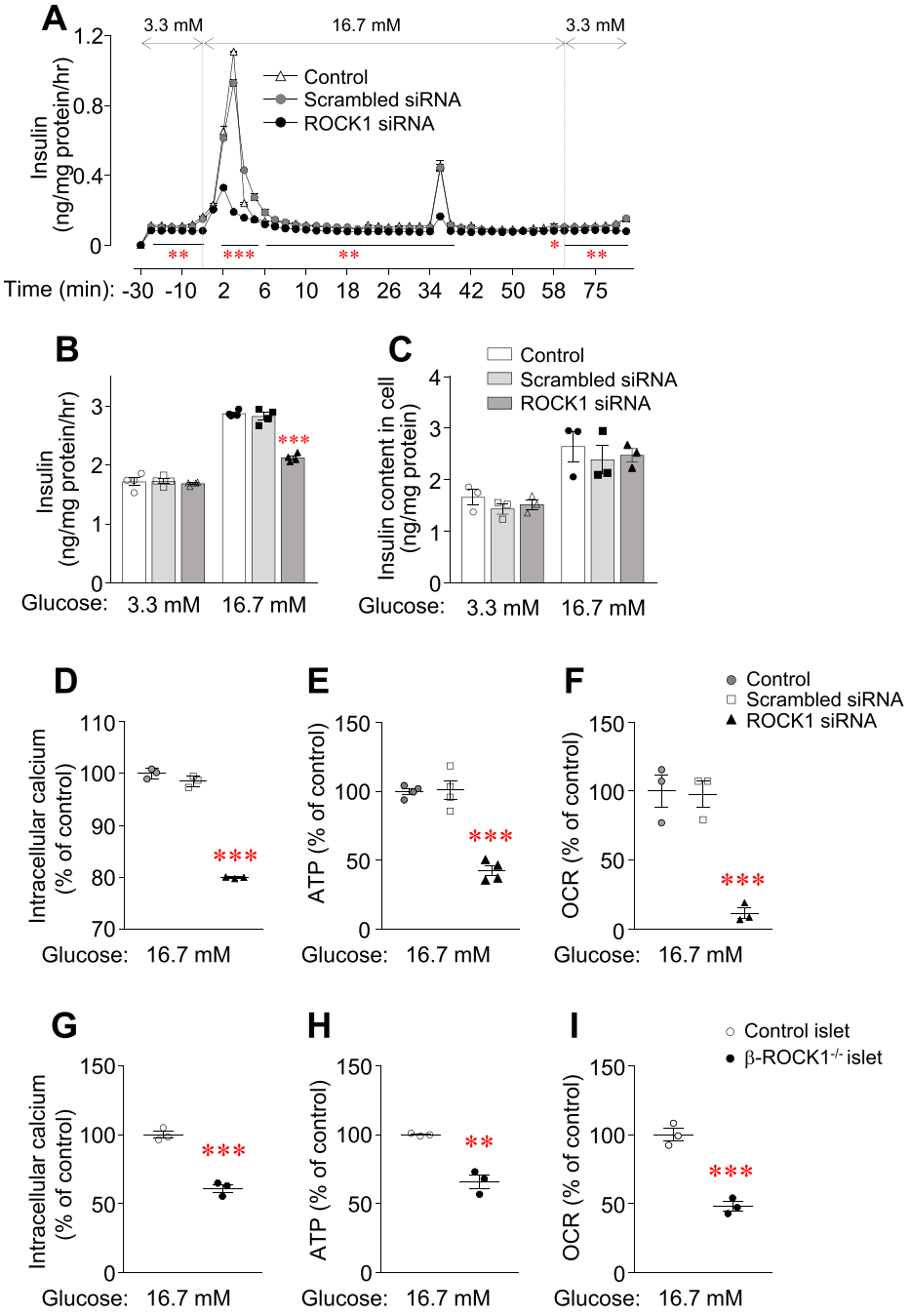

Figure 3: ROCK1 inhibition impairs glucose-stimulated insulin secretion and decreases calcium level, ATP level, and oxygen consumption rate (OCR) in INS-1 β-cells. (A) Perifusion analysis for glucose-stimulated insulin secretion (GSIS) was performed in ROCK1 knockdown INS-1 cells (n = 3). (B) GSIS (n = 4), (C) insulin content (n = 3), (D) glucose-stimulated intracellular calcium level (n = 3), (E) glucose-stimulated ATP level (n = 4), and (F) glucose-stimulated OCR (n = 3) were measured in ROCK1 knockdown INS-1 cells. (G) Glucose-stimulated intracellular calcium level (n = 3), (H) glucose-stimulated ATP level (n = 3), and (I) glucose-stimulated OCR 3 were measured in isolated islets from male control and β-ROCK1−/− mice (n = 3). Cells or islets were incubated with 16.7 mM glucose for 60 min. Thirty size-matched islets per genotype were used. N represents an individual experiment. All graphs represent means or individual values ± SEM. *p < 0.05, **p < 0.01, ***p < 0.001 vs scrambled siRNA or control islet by two-sided Student's t-test.

3.4. ROCK1 is involved in the process of insulin secretion

We measured intracellular Ca^{++} levels, ATP levels, and OCR during glucose stimulateion (16.7 mM), which are critical events associated with insulin secretion in INS-1 cells, to further investigate the underlying mechanism(s) by which ROCK1 regulates insulin secretion. siRNA-mediated inhibition of ROCK1 resulted in a significant decrease in glucose-stimulated intracellular Ca^{++} levels (Figure 3D, Supplementary Fig. 5), ATP levels (Figure 3E), as well as OCR (Figure 3F). Similar findings were observed in islets freshly isolated from β-$ROCK1^{-/-}$ mice (Figure 3G–I). These data demonstrate that ROCK1 impacts the regulatory machinery involved in insulin secretion in β-cells.

3.5. Pyruvate and PK stimulate insulin secretion in the absence of ROCK1

We further determined whether pyruvate, a key intermediate of the glycolysis pathway, is involved in insulin secretion triggered by ROCK1. Pyruvate levels greatly decreased in both INS-1 cell transfected siRNA ROCK1 and islets from β-ROCK1$^{-/-}$ mice (Figure 4A and B). Glucose-stimulated PK activity was reduced ∼15% in ROCK1 knockdown INS-1 cells compared with control cells, while fructose-1,6-bisphosphate (FBP)-induced PK activity was similar between groups (Figure 4C). Pyruvate treatment enhanced the insulin secretion in response to glucose stimulation of INS-1 β-cells transfected with scrambled siRNA. While the insulin secretion was blunted in response to glucose stimualtion in cells with ROCK1 siRNA, the insulin secretion in response to pyruvate was maintained (Figure 4D). Similar observations were found in freshly isolated islets from β-ROCK1$^{-/-}$ mice (Figure 4F). Exogenous supplementaion with pyruvate increased insulin secretion 2.9-fold in INS-1 β-cells transfected with siRNA ROCK1 and 3.3-fold in islets from β-ROCK1$^{-/-}$ mice but only 1.3-fold in INS-1 β-cells transfected with scrambled siRNA and 1.5-fold in islets from control mice (Figure 4E and G).

Similar to the effects of exogenous pyruvate, the PK activator, TEPP-46, also significantly increased GSIS in freshly isolated islets from control mice (Figure 4H). The effects of the PK activator on enhancing GSIS was evident even in the absence of ROCK1 in isolated islets (Figure 4H). Thus, the PK activator increased insulin secretion 4.8-fold in islets from β-ROCK1$^{-/-}$ mice but only 1.6-fold in islets from control mice (Figure 4I). Interestingly, glucagon-like peptide-1 (GLP-1) action was not involved in the regulation of ROCK1-mediated insulin secretion (Supplementary Fig. 6A and B). Together, these data suggest the effects of pyruvate and PK are independent of ROCK1-mediated insulin secretion in β-cells and they may play a role in regulating insulin secretion as an upstream of ROCK1.

3.6. ROCK1 interacts with pyruvate kinase

We undertook PLA, a powerful technology to detect proteins with high specificity and sensitivity, to further test the hypothesis that ROCK1 binds to PK in response to glucose [38]. PLA revealed that each red spot represents a ROCK1-PK interaction complex in INS-1 β-cells. Glucose induced a physical interaction between ROCK1 and PK in INS-1 β-cells, as evidenced by a marked increase in the number of red spots. However, this effect was significantly impaired by treatment with the ROCK inhibitor fasudil (Figure 5A). Quantitative analysis indicated that glucose stimulation increased ROCK1-PK interactions by ∼2-fold over control, and this effect was restored to control levels when ROCK inhibitor was treated (Figure 5A). These results were further confirmed in MIN6 or NIT1 β-cells (Figure 5B and C). In addition, *in vitro* overexpression studies indicated that ROCK1 binds to PK in MIN6, HEK293, or CHO cells (Figure 5D). Together, these data suggest that PK physically interacts with ROCK1 in β-cells. The precise dynamic alterations between ROCK1 and PK in disease states warrants further investigation.

4. DISCUSSION

The ability of glucose to increase insulin secretion represents a major feature of β-cell function and its dysregulation is a key pathogenic feature in all forms of diabetes [3,4]. The current study was thus designed to determine the physiological role of ROCK1 in pancreatic β-cells in homeostatic control of insulin secretion in the context of glucose metabolism. Our data clearly suggest that ROCK1 is necessary for the regulation of insulin secretion in pancreatic β-cells during glucose stimulation. This effect is likely mediated through the physical interactions between ROCK1 and PK. Thus, we identify ROCK1 as an important regulator of β-cell metabolism that may lead to new treatment options for diabetes.

A major finding of this study is that deletion of ROCK1 in pancreatic β-cells significantly decreases GSIS in vivo, which ultimately leads to systemic glucose intolerance. Studies in freshly isolated islets *ex vivo* and β-cells *in vitro* confirmed these data. Importantly, these effects are observed when insulin content or β-cell numbers are normal, suggesting that the marked reduction in insulin secretion due to ROCK1 deletion is directly linked to defects in the insulin secretory machinery rather than insulin synthesis and production. This is supported by the reduced number of insulin granules docked at the plasma membrane in β-cells from isolated islets from β-ROCK1$^{-/-}$ mice, which is associated with a decrease in the first phase of insulin release during glucose stimulation. Consistent with this view, previous reports link several proteins such as TRB3 [37], ABCA12 [39], and LKB1 [40] with modulating insulin granules and plasma membrane docking dynamics in the regulation of GSIS. The mechanism's underlying insulin granules' mobilization could involve in F-actin remodeling in response to glucose stimulation [41]. Given that ROCK regulates actin cytoskeleton reorganization [42,43], it is conceivable that ROCK1 deletion may inhibit F-actin remodeling to limit the access of insulin granules to the plasma membrane in β-cells.

The glycolytic pathway in pancreatic β-cells involves a cascade of events that break down glucose into pyruvate, producing ATP and nicotinamide adenine dinucleotide (NADH) [44]. Activation of the glycolytic pathway could lead to a significant increase in insulin secretion from β-cells. As expected, exogenous supplementation of β-cells with pyruvate greatly promotes insulin release on a background of glucose stimulation. The fact that pyruvate's ability to increase insulin secretion during glucose stimulation is enhanced in the absence of ROCK1 suggests that the ROCK1-mediated insulin secretory mechanism is linked to the actions of pyruvate. Given that pyruvate levels in islets of β-ROCK1$^{-/-}$ mice reduced, it is likely that PK, which converts phosphoenolpyruvate and ADP into pyruvate and ATP, is involved in this regulation. The significance of PK activation for the induction of insulin secretion has been recently documented [11,12]. For example, small molecule activators of PK potently amplify GSIS by switching mitochondria from oxidative phosphorylation to anaplerotic phosphoenolpyruvate biosynthesis [11]. Moreover, PK activation ameliorates GSIS in islets obtained from animals and humans, manifesting insulin resistance and type 2 diabetes [12]. In this context, we observed that treatment of ROCK1-deficient islets with the PK activator increased glucose-stimulated insulin secretion. Our data point to hypersensitization of β-cells to glucose by pyruvate or PK activator treatment in the absence of ROCK1, which leads to enhanced insulin release. Although the precise mechanism for this phenomenon remains to be elucidated, it is likely that ROCK1-deficient islets are pyruvate-sensitive. Taken together, these novel findings demonstrate that glycolytic PK signaling is linked to ROCK1 action in regulating insulin secretion.

It is useful to note that primary mouse β-cells lack the pyruvate carrier, monocarboxylate transporters (MCTs) [45]. The rescue of impaired insulin secretion by pyruvate supplementation in ROCK1 deficient b-cells may not occur directly through β-cells and could be mediated via MCTs in α-cells [46] or yet un-identified pyruvate transporters in β-cells. Further investigation is warranted to clarify the pathways that mediate pyruvate-induced insulin section on β-cells and whether MCTs are involved in this event.

Since phosphoenolpyruvate (PEP), an upstream metabolite of pyruvate, can be generated from pyruvate via PEP cycle in the mitochondria [47,48], it is likely that pyruvate regulates PK in the context of GSIS.

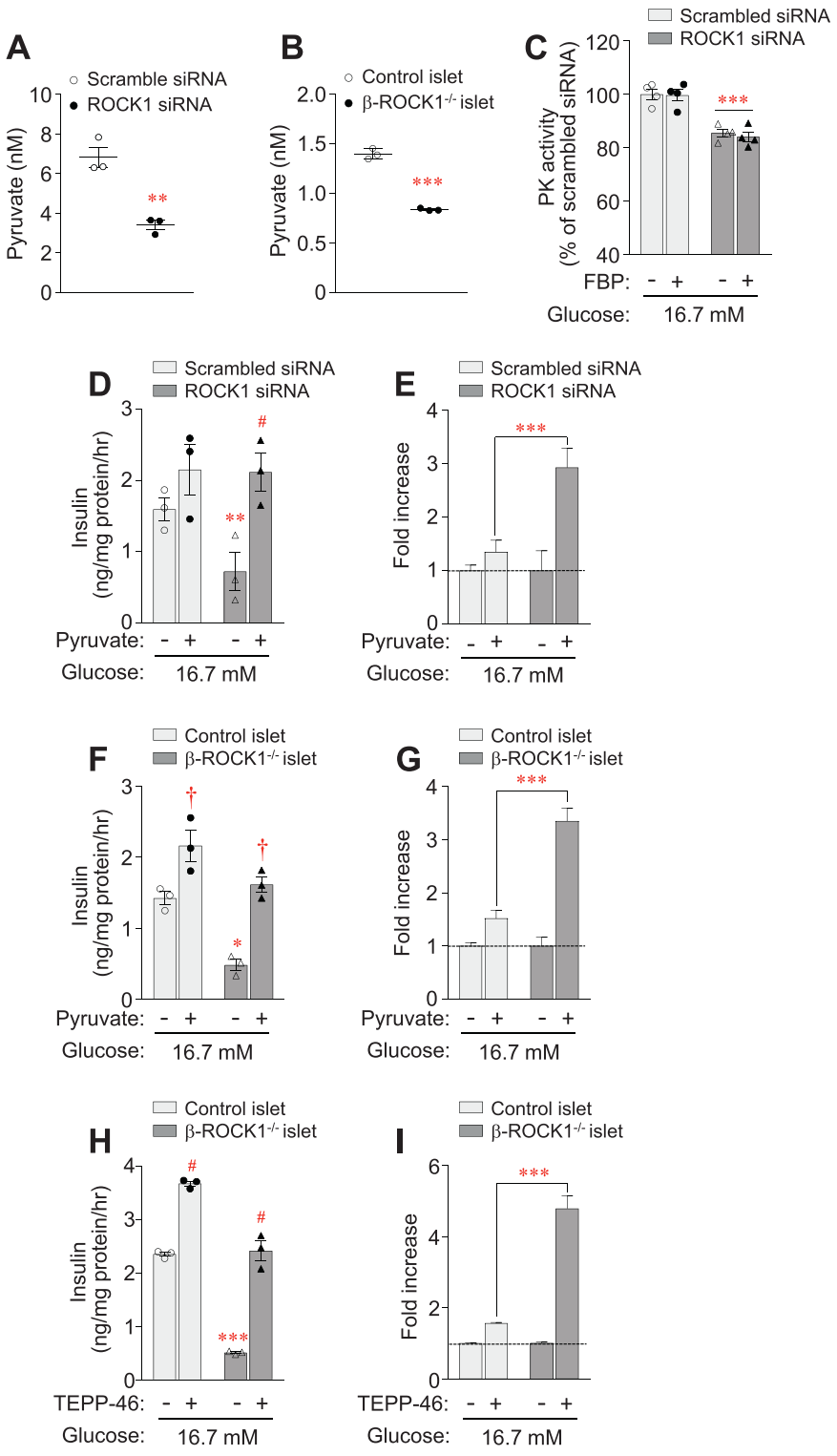

Figure 4: ROCK1 is an upstream regulator of pyruvate kinase (PK) in β-cells. Pyruvate levels were measured in (A) ROCK1 knockdown INS-1 cells (n = 3) and (B) islets from control and β-ROCK1$^{-/-}$ mice (n = 3). Cells or islets were incubated with 16.7 mM glucose for 60 min. Thirty size-matched islets per individual experiment (per genotype) were used. (C) PK activity was measured +/− fructose-1,6-bisphosphate (FBP) in ROCK1 knockdown INS-1 cells. Cells were incubated with 16.7 mM glucose for 60 min. Glucose-stimulated insulin secretion (GSIS) was measured in the absence or presence of pyruvate (10 mM) in (D) ROCK1 knockdown INS-1 cells (n = 3) and (F) islets from control and β-ROCK1$^{-/-}$ mice (n = 3). (E, G) Fold increases for GSIS were calculated from D and E, respectively. (H) GSIS was measured in the absence or presence of TEPP-46 (10 μM) in islets from control and β-ROCK1$^{-/-}$ mice (n = 3). Islets were incubated with 16.7 mM glucose for 60 min. Thirty size-matched islets per individual experiment (per genotype) were used. (I) Fold increases for GSIS were calculated from H. N represents an individual experiment. All graphs represent means or individual values ± SEM. $^{*}P < 0.05$, $^{**}P < 0.01$, $^{***}P < 0.001$ vs scrambled siRNA or control islet, $^{\S}P < 0.05$, $^{\dagger}P < 0.01$, $^{\#}P < 0.001$ vs no treatment in same group by two-sided Student's t-test or by repeated measures two-way ANOVA.

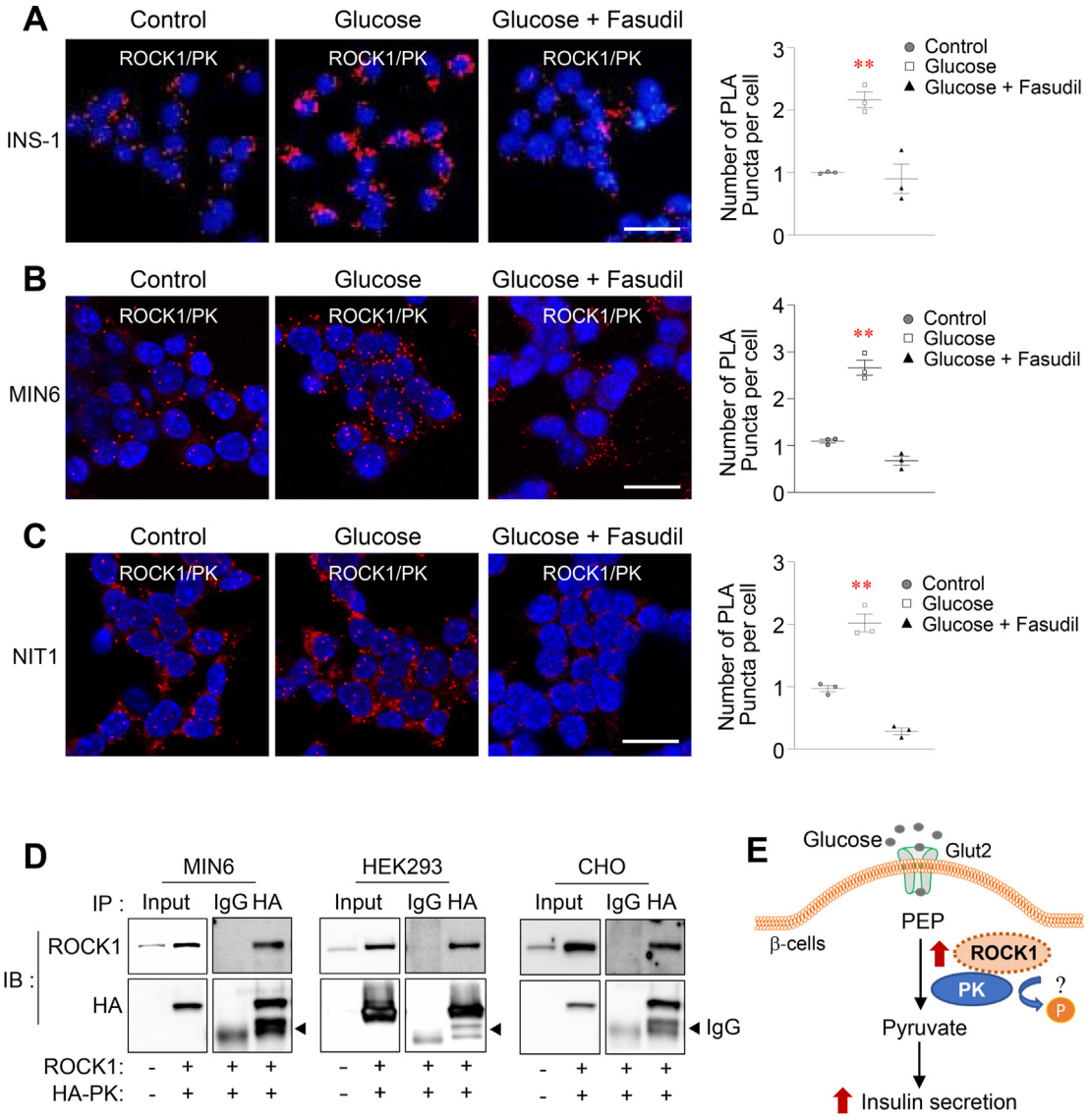

Figure 5: ROCK1 interacts with pyruvate kinase (PK) in β-cells. Proximity ligation assay (PLA) was performed in (A) INS-1, (B) MIN6, and (C) INT1 β-cells. The cells were treated with or without fasudil (10 μM) for 1 h and stimulated with high (16.7 mM) glucose for 15 min. Each red spot represents a ROCK1-PK interaction. Image data for ROCK1-PK interactions were quantitated by Image J (n = 3). N represents an individual experiment. Nuclei were stained with DAPI (blue). The scale bar represents 25 μm. (D) MIN6, HEK293, or CHO cells were transiently transfected with pAV-CAG-ROCK1 and pEGFP-C1-PKM2. The cells were harvested 48 h after transfections. Cell lysates were subjected to immunoprecipitation with IgG or HA antibody followed by immunoblotting with either ROCK1 or HA antibody. (E) Role of ROCK1 in insulin secretion in β-cells. PEP: phosphoenolpyruvate, PK: pyruvate kinase. N represents an individual experiment. All graphs represent means or individual values ± SEM. $^{**}P < 0.01$ vs control, group by two-sided Student's t-test or by repeated measures two-way ANOVA.

Thus, pyruvate supplementation is not expected to fully rescue GSIS when ROCK1-dependent PK activation is impaired. In contrast to this expectation, we observed that pyruvate treatment completely restored impaired GSIS despite impaired PK activity secondary to ROCK1 inhibition pointing to a PK-independent mechanism. A plausible explanation for this observation is the involvement of a pyruvate—malate cycle that is functionally linked to insulin secretion [49]. Malate exported from the mitochondria to the cytosol is regenerated to pyruvate by cytosolic malic enzyme for cycling back to the mitochondria [48,49]. Thus, in our studies, a pyruvate—malate cycle plays a potentially dominant role over the traditional PEP cycle in the insulin secretory regulation when pyruvate is provided in β-cells lacking ROCK1.

Our Our previous work demonstrated that global ROCK1-/mice have elevated serum insulin in the fasted and fed states owing to systemic insulin resistance. Increased insulin levels in global ROCK1−/− mice were also found during the glucose excursion of a glucose tolerance test previous work demonstrated that global ROCK1$^{-/-}$ mice exhibit elevated serum insulin owing to systemic insulin resistance [18]. It is likely the increased serum insulin in global ROCK1$^{-/-}$ mice is due to β-cell compensation for ambient insulin resistance. On the other hand, β-ROCK1$^{-/-}$ mice have lower serum insulin levels, which is due to impaired insulin secretion from β-cells. Thus, the metabolic action of ROCK1 is thought to be site- and context-dependent nature of regulation [23].

We propose that ROCK1 is a positive regulator of insulin secretion and developing small molecule for its activation may offer unexplored approaches to treating diabetes.

AUTHOR CONTRIBUTIONS

The study was designed by B.J.S., Y.B.K., and M.K.L. B.J.S., S.B.L., W.M.Y., and J.H.K. performed in vivo, *ex vivo*, and *in vitro* experiments and analyzed data. R.N.K. provided conceptual advice and contributed to the editing of the manuscript. M.K.L. and Y.B.K. wrote the manuscript with input from all other authors. M.K.L. and Y.B.K. are the senior and corresponding authors.

DATA AVAILABILITY

No data was used for the research described in the article.

ACKNOWLEDGMENTS

This work was supported by grants from Eulji University (EMBRI Grant 2021EMBRISN001 to MKL) and the National Institutes of Health (R01DK083567, R01DK129946, and R01DK123002 to YBK, and R01DK 067536 to RNK). We thank Aykut Uner for performing statistical analysis.

CONFLICT OF INTEREST

The authors have no competing interests to declare.

APPENDIX A. SUPPLEMENTARY DATA

Supplementary data to this article can be found online at https://doi.org/10.1016/j.molmet.2022.101625.

REFERENCES

[1] Divers, J., Mayer-Davis, E.J., Lawrence, J.M., Isom, S., Dabelea, D., Dolan, L., et al., 2020. Trends in incidence of type 1 and type 2 diabetes among youths - selected counties and Indian reservations, United States, 2002-2015. MMWR Morb Mortal Wkly Rep 69(6):161—165.

[2] Association, A.D., 2018. Economic costs of diabetes in the US in 2017. Diabetes Care 41(5):917—928.

[3] DeFronzo, R.A., 1997. Pathogenesis of type 2 diabetes : metabolic and molecular implications for identifying diabetes. Diabetes Rev 5:177—269.

[4] Taylor, S.I., Accili, D., Imai, Y., 1994. Insulin resistance or insulin deficiency. Which is the primary cause of NIDDM? Diabetes 43(6):735—740.

[5] Bhaswant, M., Poudyal, H., Brown, L., 2015. Mechanisms of enhanced insulin secretion and sensitivity with n-3 unsaturated fatty acids. J Nutr Biochem 26(6):571—584.

[6] de Oliveira, C.A., Latorraca, M.Q., de Mello, M.A., Carneiro, E.M., 2011. Mechanisms of insulin secretion in malnutrition: modulation by amino acids in rodent models. Amino Acids 40(4):1027—1034.

[7] Kulkarni, R.N., Bruning, J.C., Winnay, J.N., Postic, C., Magnuson, M.A., Kahn, C.R., 1999. Tissue-specific knockout of the insulin receptor in pancreatic beta cells creates an insulin secretory defect similar to that in type 2 diabetes. Cell 96(3):329—339.

[8] Withers, D.J., Gutierrez, J.S., Towery, H., Burks, D.J., Ren, J.M., Previs, S., et al., 1998. Disruption of IRS-2 causes type 2 diabetes in mice. Nature 391(6670):900—904.

[9] Prentki, M., Matschinsky, F.M., Madiraju, S.R., 2013. Metabolic signaling in fuel-induced insulin secretion. Cell Metabol 18(2):162—185.

[10] Merrins, M.J., Van Dyke, A.R., Mapp, A.K., Rizzo, M.A., Satin, L.S., 2013. Direct measurements of oscillatory glycolysis in pancreatic islet beta-cells using novel fluorescence resonance energy transfer (FRET) biosensors for pyruvate kinase M2 activity. J Biol Chem 288(46):33312—33322.

[11] Lewandowski, S.L., Cardone, R.L., Foster, H.R., Ho, T., Potapenko, E., Poudel, C., et al., 2020. Pyruvate kinase controls signal strength in the insulin secretory pathway. Cell Metabol 32(5):736—750 e735.

[12] Abulizi, A., Stark, R., Cardone, R.L., Lewandowski, S.L., Zhao, Z., Alves, T.C., et al., 2020. Pharmacologic activation of the mitochondrial phosphoenolpyruvate cycle enhances islet function in vivo. bioRxiv. https://doi.org/10.1101/2020.02.13.947630.

[13] Hu, E., Lee, D., 2005. Rho kinase as potential therapeutic target for cardiovascular diseases: opportunities and challenges. Expert Opin Ther Targets 9(4):715—736.

[14] Mishra, R.K., Alokam, R., Sriram, D., Yogeeswari, P., 2013. Potential role of rho kinase inhibitors in combating diabetes-related complications including diabetic neuropathy-A review. Curr Diabetes Rev 9(3):249—266.

[15] Hirooka, Y., Shimokawa, H., 2005. Therapeutic potential of rho-kinase inhibitors in cardiovascular diseases. Am J Cardiovasc Drugs 5(1):31—39.

[16] Begum, N., Sandu, O.A., Ito, M., Lohmann, S.M., Smolenski, A., 2002. Active Rho kinase (ROK-alpha) associates with insulin receptor substrate-1 and inhibits insulin signaling in vascular smooth muscle cells. J Biol Chem 277(8):6214—6222.

[17] Farah, S., Agazie, Y., Ohan, N., Ngsee, J.K., Liu, X.J., 1998. A rho-associated protein kinase, ROKalpha, binds insulin receptor substrate-1 and modulates insulin signaling. J Biol Chem 273(8):4740—4746.

[18] Lee, D.H., Shi, J., Jeoung, N.H., Kim, M.S., Zabolotny, J.M., Lee, S.W., et al., 2009. Targeted disruption of ROCK1 causes insulin resistance in vivo. J Biol Chem 284(18):11776—11780.

[19] Furukawa, N., Ongusaha, P., Jahng, W.J., Araki, K., Choi, C.S., Kim, H.J., et al., 2005. Role of Rho-kinase in regulation of insulin action and glucose homeostasis. Cell Metabol 2(2):119—129.

[20] Chun, K.H., Araki, K., Jee, Y., Lee, D.H., Oh, B.C., Huang, H., et al., 2012. Regulation of glucose transport by ROCK1 differs from that of ROCK2 and is controlled by actin polymerization. Endocrinology 153(4):1649—1662.

[21] Chun, K.H., Choi, K.D., Lee, D.H., Jung, Y., Henry, R.R., Ciaraldi, T.P., et al., 2012. In vivo activation of ROCK1 by insulin is impaired in skeletal muscle of humans with type 2 diabetes. Am J Physiol Endocrinol Metab 300(3):E536—E542.

[22] Huang, H., Kong, D., Byun, K., Ye, C., Koda, S., Lee, D., et al., 2012. Rho-kinase regulates energy balance by targeting hypothalamic leptin receptor signaling. Nat Neurosci 15:1391—1398.

[23] Huang, H., Lee, D.H., Zabolotny, J.M., Kim, Y.B., 2013. Metabolic actions of Rho-kinase in periphery and brain. Trends Endocrinol Metabol 24(10):506—514.

[24] Huang, H., Lee, S.H., Ye, C., Lima, I.S., Oh, B.C., Lowell, B.B., et al., 2013. ROCK1 in AgRP neurons regulates energy expenditure and locomotor activity in male mice. Endocrinology 154(10):3660—3670.

[25] Huang, H., Lee, S.H., Sousa-Lima, I., Kim, S.S., Hwang, W.M., Dagon, Y., et al., 2018. Rho-kinase/AMPK axis regulates hepatic lipogenesis during overnutrition. J Clin Invest 128(12):5335—5350.

[26] Hammar, E., Tomas, A., Bosco, D., Halban, P.A., 2009. Role of the Rho-ROCK (Rho-associated kinase) signaling pathway in the regulation of pancreatic beta-cell function. Endocrinology 150(5):2072—2079.

[27] Ono-Saito, N., Niki, I., Hidaka, H., 1999. H-series protein kinase inhibitors and potential clinical applications. Pharmacol Ther 82(2—3):123—131.

[28] Narumiya, S., Ishizaki, T., Uehata, M., 2000. Use and properties of ROCK-specific inhibitor Y-27632. Methods Enzymol 325:273—284.

[29] Diep, D.T.V., Hong, K., Khun, T., Zheng, M., Ul-Haq, A., Jun, H.S., et al., 2018. Anti-adipogenic effects of KD025 (SLx-2119), a ROCK2-specific inhibitor, in 3T3-L1 cells. Sci Rep 8(1):2477.

[30] Alquier, T., Poitout, V., 2018. Considerations and guidelines for mouse metabolic phenotyping in diabetes research. Diabetologia 61(3):526—538.
[31] Lacy, P.E., Kostianovsky, M., 1967. Method for the isolation of intact islets of Langerhans from the rat pancreas. Diabetes 16(1):35—39.
[32] Ni, N.C., Yan, D., Ballantyne, L.L., Barajas-Espinosa, A., St Amand, T., Pratt, D.A., et al., 2011. A selective cysteinyl leukotriene receptor 2 antagonist blocks myocardial ischemia/reperfusion injury and vascular permeability in mice. J Pharmacol Exp Therapeut 339(3):768—778.
[33] Lamb, R., Fiorillo, M., Chadwick, A., Ozsvari, B., Reeves, K.J., Smith, D.L., et al., 2015. Doxycycline down-regulates DNA-PK and radiosensitizes tumor initiating cells: implications for more effective radiation therapy. Oncotarget 6(16):14005—14025.
[34] Seo, J.A., Kang, M.C., Yang, W.M., Hwang, W.M., Kim, S.S., Hong, S.H., et al., 2020. Apolipoprotein J is a hepatokine regulating muscle glucose metabolism and insulin sensitivity. Nat Commun 11(1):2024.
[35] Gomi, H., Mizutani, S., Kasai, K., Itohara, S., Izumi, T., 2005. Granuphilin molecularly docks insulin granules to the fusion machinery. J Cell Biol 171(1): 99—109.
[36] Rorsman, P., Renstrom, E., 2003. Insulin granule dynamics in pancreatic beta cells. Diabetologia 46(8):1029—1045.
[37] Liew, C.W., Bochenski, J., Kawamori, D., Hu, J., Leech, C.A., Wanic, K., et al., 2010. The pseudokinase tribbles homolog 3 interacts with ATF4 to negatively regulate insulin exocytosis in human and mouse beta cells. J Clin Invest 120(8):2876—2888.
[38] Soderberg, O., Gullberg, M., Jarvius, M., Ridderstrale, K., Leuchowius, K.J., Jarvius, J., et al., 2006. Direct observation of individual endogenous protein complexes in situ by proximity ligation. Nat Methods 3(12):995—1000.
[39] Ursino, G.M., Fu, Y., Cottle, D.L., Mukhamedova, N., Jones, L.K., Low, H., et al., 2020. ABCA12 regulates insulin secretion from beta-cells. EMBO Rep 21(3):e48692.
[40] Fu, A., Robitaille, K., Faubert, B., Reeks, C., Dai, X.Q., Hardy, A.B., et al., 2015. LKB1 couples glucose metabolism to insulin secretion in mice. Diabetologia 58(7):1513—1522.
[41] Kalwat, M.A., Thurmond, D.C., 2013. Signaling mechanisms of glucose-induced F-actin remodeling in pancreatic islet beta cells. Exp Mol Med 45:e37.
[42] Iizuka, M., Kimura, K., Wang, S., Kato, K., Amano, M., Kaibuchi, K., et al., 2012. Distinct distribution and localization of Rho-kinase in mouse epithelial, muscle and neural tissues. Cell Struct Funct 37(2):155—175.
[43] Kawano, Y., Fukata, Y., Oshiro, N., Amano, M., Nakamura, T., Ito, M., et al., 1999. Phosphorylation of myosin-binding subunit (MBS) of myosin phosphatase by Rho-kinase in vivo. J Cell Biol 147(5):1023—1038.
[44] Sugden, M.C., Holness, M.J., 2011. The pyruvate carboxylase-pyruvate dehydrogenase axis in islet pyruvate metabolism: going round in circles? Islets 3(6):302—319.
[45] Zhao, C., Wilson, M.C., Schuit, F., Halestrap, A.P., Rutter, G.A., 2001. Expression and distribution of lactate/monocarboxylate transporter isoforms in pancreatic islets and the exocrine pancreas. Diabetes 50(2):361—366.
[46] Zaborska, K.E., Dadi, P.K., Dickerson, M.T., Nakhe, A.Y., Thorson, A.S., Schaub, C.M., et al., 2020. Lactate activation of alpha-cell KATP channels inhibits glucagon secretion by hyperpolarizing the membrane potential and reducing Ca(2+) entry. Mol Metabol 42:101056.
[47] Stark, R., Kibbey, R.G., 2014. The mitochondrial isoform of phosphoenolpyruvate carboxykinase (PEPCK-M) and glucose homeostasis: has it been overlooked? Biochim Biophys Acta 1840(4):1313—1330.
[48] Cline, G.W., 2011. Fuel-stimulated insulin secretion depends upon mitochondria activation and the integration of mitochondrial and cytosolic substrate cycles. Diabetes Metab J 35(5):458—465.
[49] Pongratz, R.L., Kibbey, R.G., Shulman, G.I., Cline, G.W., 2007. Cytosolic and mitochondrial malic enzyme isoforms differentially control insulin secretion. J Biol Chem 282(1):200—207.

